Transportation of granular materials with ultrasonic augers

Xuan Li
Centre for Medical & Industrial Ultrasonics, James Watt School of Engineering
University of Glasgow
Glasgow, UK
Xuan.Li@glasgow.ac.uk

Xiaoniu Li
State Key Lab of Mechanics and Control of Mechanical Structures
Nanjing University of Aeronautics and Astronautics
Nanjing, China
lixiaoniu@nuaa.edu.cn

Tianlu Huang
State Key Lab of Mechanics and Control of Mechanical Structures
Nanjing University of Aeronautics and Astronautics
Nanjing, China
huangtianlu@nuaa.edu.cn

Andrew Feeney
Centre for Medical & Industrial Ultrasonics, James Watt School of Engineering
University of Glasgow
Glasgow, UK
Andrew.Feeney@glasgow.ac.uk

Kevin Worrall
Centre for Medical & Industrial Ultrasonics, James Watt School of Engineering
University of Glasgow
Glasgow, UK
Kevin.Worrall@glasgow.ac.uk

Patrick Harkness
Centre for Medical & Industrial Ultrasonics, James Watt School of Engineering
University of Glasgow
Glasgow, UK
Patrick.Harkness@glasgow.ac.uk

***Abstract*—Drilling extra-terrestrial planets can be difficult, which is restrained by the payloads, power, and requirements of low axial force of rover posed by low environmental gravity, and drill bits can be trapped at a large depth, due to the accumulated spoils resulted from the low efficiency removal rate. This can cause motor to stall and draw excessive power. This work explores the opportunity of superposition of ultrasonic vibration on a vertical rotating auger in a variety of granular media. Ultrasonic vibration is known to facilitate direct penetration of granular materials, and it is anticipated that any related reduction in the contact friction force might improve augering performance.**

Experimental results suggest that, compared to the non-ultrasonic scenario, ultrasonically assisted augering process has significantly promoted the flow of granular media and has moderately reduced the torque required to operate the device. Furthermore, it was discovered that particle size and auger speed also affect the performance of the auger system in different ways as the ultrasonic amplitude is adjusted.

Keywords—Ultrasonically assisted auger, torque, granular material

I. INTRODUCTION

Ultrasonic vibration as a penetration aid with respect to granular materials was first explored in some detail in 2017 [1], when it was demonstrated that the forces required to access the near subsurface could be substantially reduced. The proximate application was considered to be planetary exploration, where reduced forces could make it easier for probes to explore the dusty regolith of planets, moons, and asteroids.

However, it may be necessary to explore beneath rocky terrain as well, which requires drill systems to break the harder material. In every drill used in space to date, the rock breaking function has been combined with an auger to elevate the spoil out of the hole. This paper will explore whether sonication could similarly enhance the flow of spoil up such an auger, and therefore contribute to exploration of these more challenging terrains by reducing the effort required to rotate the drillstring. This would be particularly applicable for drillstrings less than a few wavelengths long.

Such an outcome was considered possible because of the manner in which augers work: the low friction of the flights causes the spoil to preferentially slide up the scroll, rather than rotate against the high frictional forces of the borehole wall [2]. If the reduced forces seen in penetration can be similarly leveraged in a rotating system, then this effect should be supported and the auger should operate more effectively, and this study confirms that such effect exists.

II. MATERIAL AND METHODS

A. Granular material

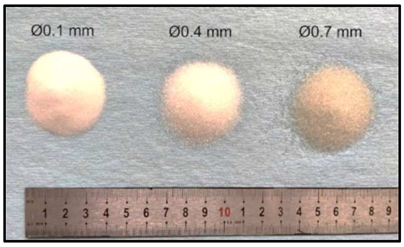

Fig. 1. Three different diameters of glass beads, used as granular materials for experimental purposes

The spoil created during actual drilling may have a wide range of properties, so for the purposes of this experiment a highly repeatable substitute is used. Three batches of glass beads, with approximate diameters of 0.1 mm, 0.4 mm and 0.7 mm, are used, shown in Fig. 1.

B. Ultrasonic auger system

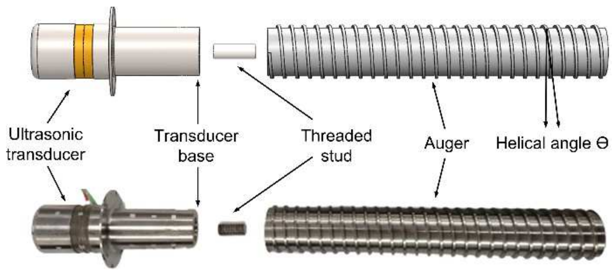

Fig. 2. 5° helical angle ultrasonic auger model and real device as manufactured

The research was supported by the "Ultrasonically Assisted Augers" project from the UK Space Agency

Fig. 2 shows the structure of the ultrasonic auger, as part of a Bolted Langevin Transducer (BLT) architecture. This configuration is comprised of a half-wavelength ultrasonic transducer (model number L500, Sonic Systems Ltd, Puckington, Ilminster, UK) tuned to resonate at its first longitudinal mode (L1) at around 20 kHz. A cylindrical auger (made from Ti-6Al-4V material), with a helix angle of 5°, was designed using the finite element analysis (FEA) software package Abaqus-Simulia (Dassault Systèmes, Vélizy-Villacoublay, France), manufactured, tuned to the full-wavelength, and then interfaced so that it can be attached to the transducer by means of a threaded stud. This forms a one-and-a-half wavelength device, resonating at around 20 kHz overall. The diameter of the cylindrical core of the auger is 34 mm, matching the diameter of the transducer, and the outer diameter (across the auger scrolls) is 38 mm.

III. Experimental plarform

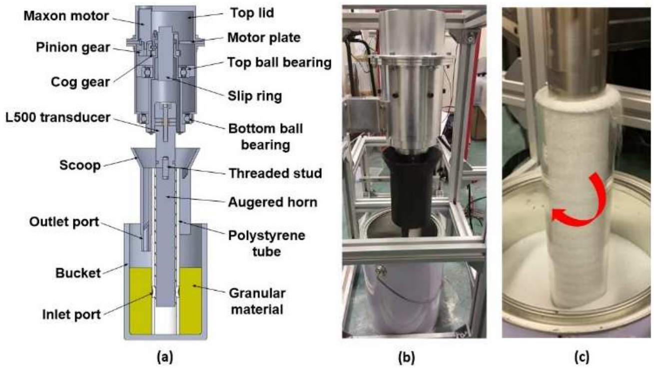

Fig. 3. (a) cross-sectional view of the experimental plarform of the ultrasonic auger system, (b) real experimental setup, (c) ultrasonically assisted auger in operation, with the media overtopping the tube (the scoop is not present)

The experimental platform is presented in Fig. 3 (a). The ultrasonic stack is fixed to a spun housing through its nodal flange, with two contact bearings supporting the assembly. A cog gear is seated on the upper shoulder of the transducer housing, where it can be driven by a small pinion and a gearmotor (Maxon Group, Sachsein, Switzerland). To supply power to the spun assembly, a slip ring (MFS028-P0210-440V, Moflon Technology, Shenzhen, China) is used. A benchtop power supply (BK9129B, BK Precision, Yorba Linda, CA, USA) provides this power, with the power consumption of the gearmotor being recorded using an associated kit (IT-E132B) and LabView program.

A bucket with granular media (shown in Fig. 1) is deployed directly underneath the ultrasonic auger. A transparent polystyrene tube is placed concentrically around the auger and is inserted in the granular material, to the bottom of the bucket, to help stabilise the auger against oscillation and whirl. The tube has an inner diameter of 40 mm, leaving a 1 mm circumferential gap, and it has two 20 mm diameter holes at the sides which act as inlet ports. A scoop made from polylactic acid is press fitted to the top of the tube, with an inclined surface that enables any material lifted by the auger to be directed in a spout where it may be collected for transfer to a digital scale. In this way, the mass uplifted by the auger during any given run-time of the experiment may be recorded.

Fig. 3 (b) and (c) illustrate the experimental platform while the auger system is in operation. The red arrow indicates the direction of the rotation of the auger.

To energise the ultrasonic augers, a P100 control unit (Sonic Systems Ltd, Puckington, Ilminster, UK) is used. This vibration control unit employs a resonant frequency tracking technique [3], which automatically adjusts the output frequency to precisely match the resonance of the augers. A negative feedback control loop is integrated in the P100 control unit to maintain a constant displacement amplitude of the augers under load. The ultrasonic power consumption can be acquired from the P100 control unit.

IV. Results

A. *Electromechanical characteristics of the auger*

To ensure the ultrasonic auger can be driven by the P100 control unit under load (with the surrounding granular materials), the electromechanical characteristics will need to be confirmed.

1) *Electrical impedance*

Impedance analysis (IA) measurements was performed on the ultrasonic auger using a commercial device (4294A, Agilent Technologies, Santa Clara, CA, USA). A swept signal of 1 V peak-to-peak over a bandwidth covering the frequency range of interest was applied, and the impedance spectrum was measured. The effective electromechanical coupling coefficient, k_{eff}, was calculated from the impedance spectrum data using equation (1) [4], providing an understanding of the ultrasonic auger's conversion efficiency from electrical energy to mechanical vibrations.

$$k_{eff}^2 = \frac{f_a^2 - f_r^2}{f_a^2} \quad (1)$$

f_a represents the anti-resonant frequency and f_r stands for the resonant frequency.

Mechanical Q factor was also calculated from the impedance measurements, to understand the damping of the system. However, it must be noted that this value can change with excitation level.

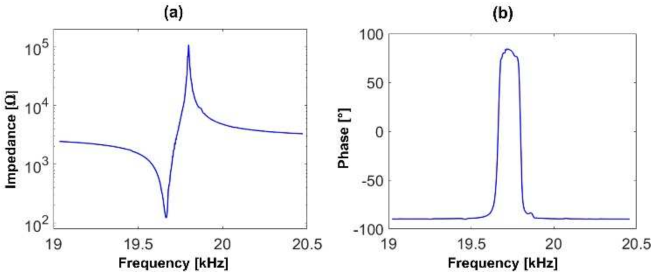

Fig. 4. Measured electrical impedance and phase of the ultrasonic auger: (a) impedance, (b) phase

TABLE I. Ultrasonic auger electrical characteristics

Resonance frequency f_r [Hz]	19666
Anti-resonance frequency f_a [Hz]	19799
Impedance magnitude Z [Ω]	123
Phase θ at f_r [°]	18.5
Coupling coefficient K_{eff} [-]	0.117
Q factor [-]	1093

The experimentally measured impedance and phase curves of the auger are shown in Fig. 4, with the calculated electrical characteristics presented in Table I. The resonance frequency shows a value within the tracking range of 19.5 to 20.5 kHz, where the resonance can be maintained by the P100 control system. Also, the impedance magnitude value is between 100 Ω to 150 Ω, close to the output impedance of the P100 control unit (50 Ω), to ensure maximum energy transfer. Electromechanical coupling coefficient value is 0.117, and finally, Q factor value is around 1100, demonstrating a low loss in the system as manufactured.

2) Experimental modal analysis

Experimental modal analysis (EMA) was performed to confirm the consistency of the vibration mode shapes with the theoretical design. Frequency response functions (FRFs) were taken across a grid of vibration response measurement points, from which the modal parameters (frequency, damping, and mode shape) were extracted [5].

To generate the FRFs, a white noise excitation signal of 10 V_{rms} was generated by a signal generator (Quattro, Data Physics, Santa Clara, CA, USA) and amplified by a power amplifier (RMX 4050HD, QSC Audio Products, Costa Mesa, CA, USA), before being supplied to the ultrasonic auger. A 3-D laser Doppler vibrometer (CLV3000, Polytec, Waldbronn, Germany) was used to measure three orthogonal components of the vibrational velocities from the grid points. Data acquisition and processing software (SignalCalc, Data Physics, Santa Clara, CA, USA) was then used to apply curve-fitting routines to extract the magnitude and phase data. Finally, the measured FRFs were exported to modal analysis software (ME'scopeVES, Vibrant Technology Inc, Centennial, CO, USA) to extract the modal parameters.

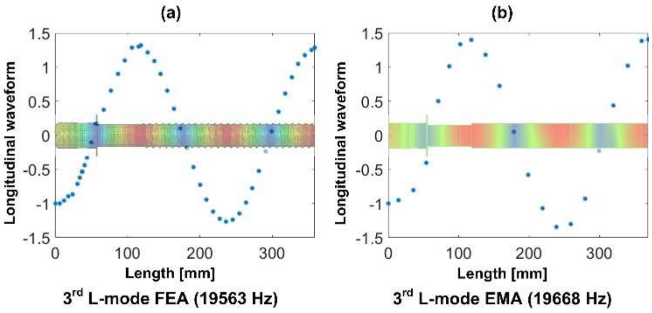

Fig. 5. Simulated and measured vibration mode shapes and longitudinal waveforms of the ultrasonic auger: (a) FEA modeshape, (b) EMA modeshape

The simulated and experimentally identified vibration mode shapes for the ultrasonic auger at its one-and-half wavelength longitudinal mode are presented in Fig. 5.

Operating at the third longitudinal mode (L3), the auger presents three nodes, located at the flange of the L500 transducer (allowing the ultrasonic stack to be clamped), and at roughly quarter-distance points from both ends of the actual auger. Amplification gain values (defined as the ratio of the displacement amplitude at the front face of the auger and end face of the back mass) is 1.29 from FEA prediction, and 1.41 from EMA measurement. Resonance frequencies are all around 19.6 kHz for both simulation and experiment.

B. Final setup for the ultrasonic augering experiment

Now that the ultrasonic auger system has been fully characterised, it can be used in the experiment.

Three buckets of granular materials with diameters of 0.1 mm, 0.4 mm, and 0.7 mm were prepared for the experiment (see Fig. 3 (b)). Displacement amplitudes at the base of the ultrasonic transducer were set to 0 µm (non-ultrasonic), 5 µm and 10 µm, amplified by a gain of 1.4 (see Fig. 5) to achieve a slightly higher amplitude at the front face of the auger. After a few exploratory runs, rotational speeds of 96 rpm, 144 rpm, and 192 rpm were selected. Each uplift cycle ran for 30 seconds and was repeated three times. Average output parameters of the system, such as mass uplifted in grams and motor power consumption were recorded. Finally, the torque exerted on the auger system was calculated using equation (2), where T is the torque in Nm, P is power in Watt, and V is the rotational speed of the motor in rpm.

$$T = \frac{9548.8P}{V} \tag{2}$$

C. Mass flow

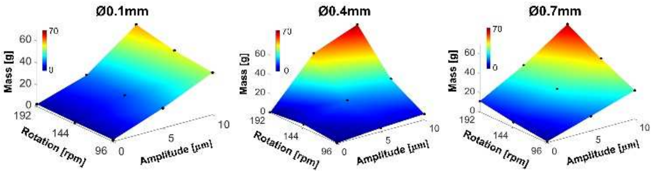

Fig. 6. Collected mass over 30 seconds, for three diameters granular medium, as a function of excitation amplitude and rotational speed. Each datapoint is the average of three experimental runs.

The mass of material uplifted over 30 seconds is presented in Fig. 6. In general, when operating at a larger displacement amplitude, more granular material was transported.

It was more challenging to sustain uplift in finer materials, the 0.7 mm material appeared to be facilitated by ultrasonic excitation to the greatest degree, with sonication reducing the grinding noise heard in the unsonicated cases and generally providing a more fluid-like appearance through the sides of the transparent tube. This noise was likely generated by the larger individual particles becoming trapped between the auger and the tube.

D. Motor power

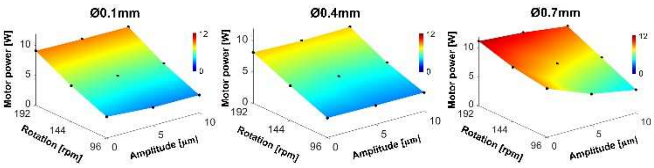

Fig. 7. Average motor power, for three diameters granular medium, as a function of excitation amplitude and rotational speed. Each datapoint is the average of three experimental runs.

It was anticipated that ultrasonic vibration would reduce the rotational power requirement, and this effect is indeed observed in Fig. 7. It appears most strongly when operating at the lowest speeds, in the coarsest materials: the auger in the 0.7 mm material sees a reduction in motor power of 14%, 27%, and 52% for the 192 rpm, 144 rpm, and 96 rpm cases as displacement amplitude rises from 0 µm to 5 µm, and then to 10 µm.

E. Motor torque

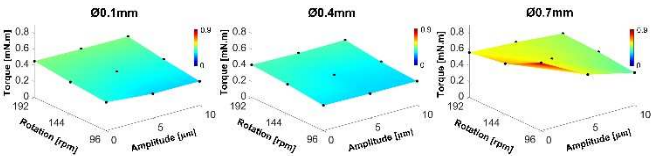

Fig. 8. Torque, for three diameters granular medium, as a function of excitation amplitude and rotational speed. Each datapoint is the average of three experimental runs.

Using equation (2) and the motor power consumption values shown in Fig. 7, the torque exerted on the auger can be estimated. The results are presented in Fig. 8.

As was the case in the motor power analysis, the advantages of ultrasonic vibration are most strongly felt when the auger is operated at the lowest speeds, in the coarsest materials. Under these circumstances, auger torque reductions on the order of 50% are possible.

V. Discussion

The effects observed in this study are believed to be associated with ultrasonically enhanced fluidization in the space between the auger and the surrounding auger tube, and in particular, a reduction in the friction at the auger surface itself.

Any granular material satisfies some of the basic qualitative criteria for 'liquidity'. Such materials will fill a container, but they can also maintain internal shear stresses, which is why they can cause an auger to seize. This is possible because stable chains of relatively few contacting particles can form dendritic patterns to transmit force into the far-field [6]. However, like mayonnaise, this solidity can give way to a viscous fluid-like behaviour at higher stress. The transition is more complex though, because in mayonnaise (a Bingham plastic) this occurs at an absolute yield stress, but in granular media the breakdown (unjamming) is friction based [7], and influenced by pressure and particle shape [8]. It can also, apparently, be triggered by ultrasonic vibration [9].

VI. Conclusion

The application of ultrasonic vibration to an auger has been shown to have a positive effect on the rate of material throughput and the torque requirements of the system. This effect appears to be most significant when the auger is being rotated at the lower end of its operational speed band.

It is suspected that the mechanism is connected to a reduction in the effective friction coefficient of the auger scrolls against the granular material, which may in turn be connected to the fluidization effects of the ultrasonic vibration in the near-field.

The effect itself is consistent and repeatable, and it has particular applicability in shallow drill systems that require drill bits no longer than a few hundred mm, which could conceivably be engineered to resonate in a similar manner to the experimental rigs described herein.

Acknowledgment

The authors acknowledge the kind support of the UK Space Agency in the "Ultrasonically Assisted Augers" project.

References

[1] D. Firstbrook, K. Worrall, R. Timoney, F. Suñol, Y. Gao, and P. Harkness, "An experimental study of ultrasonic vibration and the penetration of granular material," *Proceedings of the Royal Society A: Mathematical, Physical and Engineering Sciences*, vol. 473, no. 2198, 2017.

[2] K. Zacny and G. Cooper, "Methods for cuttings removal from holes drilled on Mars," *Mars, The International Journal of Mars Science and Exploration*, vol. 3, pp. 42–56, 2007.

[3] V. I. Babitsky, A. N. Kalashnikov, and F. V. Molodtsov, "Autoresonant control of ultrasonically assisted cutting," *Mechatronics*, vol. 14, no. 1, pp. 91–114, 2004.

[4] A. Caronti, R. Carotenuto, and M. Pappalardo, "Electromechanical coupling factor of capacitive micromachined ultrasonic transducers," *The Journal of the Acoustical Society of America*, vol. 113, no. 1, pp. 279–288, 2003.

[5] P. Avitabile, "Experimental Modal Analysis," *Sound and Vibration Magazine*, vol. 35, no. 1, pp. 1–15, 2001.

[6] J. F. Peters, M. Muthuswamy, J. Wibowo, and A. Tordesillas, "Characterization of force chains in granular material," *Physical Review E*, *The American Physical Society*, vol. 72, no. 4, pp. 1–8, 2005.

[7] O. Reynolds, "On the dilatancy of media composed of rigid particles in contact, with experimental illustrations," *Philosophical magazine and journal of science, fifth series*, vol. 20, no. 127, pp. 469–481, 1885.

[8] L. Staron, P. Y. Lagrée, P. Ray, and S. Popinet, "Scaling laws for the slumping of a Bingham plastic fluid," *Journal of Rheology*, vol. 57, no. 4, pp. 1265–1280, 2013.

[9] A. Feeney, S. Sikaneta, P. Harkness, and M. Lucas, "Ultrasonic compaction of granular geological materials," *Ultrasonics*, vol. 76, pp. 136–144, 2017.